

TABLE 25. PREDICTIVE EQUATIONS FOR ^{iv}Al IN THE *Prima* AMPHIBOLES

$Al^{TOT} = -26.368 + 16.252 << T-O >>$	
T1A $Al = -13.146 + 8.126 < T1A-O >$	T2A $Al = -13.175 + 8.126 < T2A-O >$
T1B $Al = -13.157 + 8.126 < T1B-O >$	T2B $Al = -13.257 + 8.126 < T2B-O >$

$$Al = ^{iv}Al \text{ p.f.u./4.0}$$

were assigned by assuming linearity between holmquistite[31] and gedrite[33] in Figure 41, with the exception of T2A, for which gedrite[32] was assumed to have zero Al occupancy. The site occupancies assigned for anthophyllite[23] and gedrite[32] are supported by the fact that the total site-chemistry agrees with the corresponding values derived from the chemical analysis (anthophyllite[23]) and estimated from the refined value of the A-site Na (gedrite[32]). In view of the limited data-set, regression analyses were not performed; preliminary working-curves (Fig. 41) were derived by shifting the monoclinic amphibole curves down to correspond to the orthorhombic data to give the equations listed in Table 25.

All the methods outlined above have depended on ionic size as a criterion for the detection of Al/Si ordering. However, the bond-strength curves of Brown & Shannon (1973) may be used to assign site occupancies, and good agreement with the results of neutron diffraction experiments were obtained for sanidine (Brown & Shannon 1973, p. 277). As a part of this study, this approach was tried for the amphiboles of Appendices B and C, with the total amount of tetrahedral Al indicated by the chemical analysis as a check on the total tetrahedral Al indicated by the bond-valence calculations. Using the universal curves of Brown & Shannon (1973), the agreement was found to be poor; the tetrahedral Al was overestimated [*e.g.*, obs = 0.34, calc = 0.62 atoms p.f.u. for manganian ferroactinolite(37); obs = 2.73, calc = 3.57 atoms p.f.u. for subsilicic titanian magnesian hastingsite(58)] and in synthetic nonaluminous amphiboles, up to 0.38 Al p.f.u. [fluor-richterite(34)] was calculated. Results were improved somewhat by the use of the "co-ordination corrected" curves of Brown & Shannon (1973). However, co-ordination numbers are sometimes difficult to decide convincingly, particularly when the next-nearest-neighbor cations are positionally disordered, the site is only partly occupied and the bonding contacts are at the margin of significance. In view of the reasonably satisfactory nature of the bond length vs. occupancy

curves given above, this approach was not pursued further.

Stereochemistry of the double chain

As was shown in the previous section on model structures, increasing substitution of Al at the tetrahedral sites is accompanied by increased rotation of the tetrahedra of the double chain toward an O-rotated configuration in order to maintain linkage between the tetrahedral chain and octahedral strip parts of the structure. Substitution of Al at the tetrahedral sites is accompanied by balancing substitutions in other parts of the structure. The combination of these substitutions must be accompanied by stereochemical adjustments that allow the bond-valence requirements of the anions to be satisfied. The way in which this is done is apparent from the bond-valence tables for selected amphiboles shown in Table 26. The discussion on bond-length variations in non- ^{iv}Al amphiboles emphasized the role of the O(4) anion; it is apparent from Table 26 that the same bond-valence constraints are operative in the ^{iv}Al amphiboles. Bond valences to the O(4) anion must be maintained at high values; thus ^{iv}Al will tend to avoid sites bonded to O(4) and order at sites not bonded to O(4). This is the case in the amphiboles of Table 26, where it can be seen that the bond valence of the T(2)-O(4) bond is the largest in the structure of each amphibole. The decrease in bond valence contributed to the anions co-ordinating the T(1) site is compensated for by the substitution of higher-valence cations at the other sites co-ordinated to these anions, and also by a strengthening of the M(4)-O(br) bonds that is promoted by the increased O-rotation of the double chain described above.

THE OCTAHEDRAL STRIP

Sandwiched between opposing tetrahedral double-chains is the octahedral strip, an array of pseudo-octahedrally co-ordinated cation sites that are occupied by the C-type cations of the formula unit. This is the most compliant part of the amphibole structure, accepting cations that

TABLE 26. EMPIRICAL BOND-VALENCE (V.U.) TABLES FOR SELECTED ALUMINOUS $C2/m$ AMPHIBOLES

M(1)	M(2)	M(3)	M(4)	A	T(1)	T(2)	Σ	Σ^P
Potassium pargasite (38): r.m.s. deviations are 4.0% and 9.8% respectively								
0(1)	0.377	0.372	0.362 $\frac{X^2}{2}$		0.898		2.009	1.991
0(2)	0.335	0.368	0.282		0.977	0.977	1.962	1.981
0(3)	0.345 $\frac{X^2}{2}$	0.358			1.048		1.048	1.000
0(4)	0.473	0.473	0.320		1.038	1.831	1.648	1.648
0(5)			0.179	0.065 $\frac{X^2}{2}$	0.832	0.949	2.025	2.226
0(6)			0.204	0.095 $\frac{X^2}{2}$	0.856	0.901	2.056	2.226
0(7)				0.210	0.898 $\frac{X^2}{2}$		2.006	1.903
Σ	2.114	2.425	2.164	1.970	1.060	3.484	3.865	
Ferro-tschermakite (54): r.m.s. deviations are 3.7% and 8.1% respectively								
0(1)	0.393	0.421	0.336 $\frac{X^2}{2}$		0.887		2.037	2.029
0(2)	0.307	0.407	0.277		0.954	0.954	1.945	2.040
0(3)	0.337 $\frac{X^2}{2}$	0.357			1.031		1.031	1.000
0(4)	0.517	0.517	0.332		1.005	1.854	1.707	1.707
0(5)			0.171	0.018 $\frac{X^2}{2}$	0.834	0.964	1.987	2.159
0(6)			0.219	0.015 $\frac{X^2}{2}$	0.862	0.915	2.011	2.159
0(7)				0.076	0.915 $\frac{X^2}{2}$		1.906	1.815
Σ	2.074	2.690	2.058	1.998	0.284	3.498	3.838	
Potassium ferri-taramite (59): r.m.s. deviations are 3.1% and 8.8% respectively								
0(1)	0.395	0.391	0.353 $\frac{X^2}{2}$		0.892		2.031	2.036
0(2)	0.324	0.406	0.230		0.979	0.979	1.939	2.006
0(3)	0.357 $\frac{X^2}{2}$	0.365			1.079		1.079	1.000
0(4)	0.616	0.616	0.265		1.049	1.930	1.673	1.673
0(5)			0.130	0.073 $\frac{X^2}{2}$	0.854	0.939	1.996	2.188
0(6)			0.185	0.055 $\frac{X^2}{2}$	0.860	0.910	2.010	2.188
0(7)				0.243	0.896 $\frac{X^2}{2}$		2.035	1.885
Σ	2.152	2.826	2.142	1.620	0.998	3.502	3.876	
Clinoholmquistite (62): r.m.s. deviations are 13.4% and 10.5% respectively								
0(1)	0.314	0.454	0.370 $\frac{X^2}{2}$		1.060		2.198	2.216
0(2)	0.384	0.416	0.105		0.778	0.778	1.683	1.967
0(3)	0.367 $\frac{X^2}{2}$	0.467			1.201		1.201	1.049
0(4)	0.569	0.569	0.164		1.060	1.793	1.634	1.634
0(5)			0.063	0.070 $\frac{X^2}{2}$	0.838	1.120	2.091	2.193
0(6)			0.208	0.029 $\frac{X^2}{2}$	1.215	0.954	2.377	2.193
0(7)				0.126	1.032 $\frac{X^2}{2}$		2.190	2.059
Σ	2.130	2.878	2.414	1.080	0.532	4.145	3.912	
Potassium-arfvedsonite (67): r.m.s. deviations are 4.8% and 11.4% respectively								
0(1)	0.373	0.329	0.347 $\frac{X^2}{2}$		1.066		2.115	2.104
0(2)	0.383	0.401	0.188		1.019	1.019	1.991	1.906
0(3)	0.349 $\frac{X^2}{2}$	0.379			1.077		1.077	1.000
0(4)	0.574	0.574	0.204		1.104	1.862	1.573	1.573
0(5)			0.080	0.154 $\frac{X^2}{2}$	0.969	0.889	2.092	2.235
0(6)			0.133	0.047 $\frac{X^2}{2}$	0.974	0.860	2.014	2.235
0(7)				0.227	0.951 $\frac{X^2}{2}$		2.129	2.100
Σ	2.210	2.608	2.146	1.210	1.258	3.960	3.872	
Magnesio-hornblende (45): r.m.s. deviations are 4.0% and 9.9% respectively								
0(1)	0.385	0.354	0.364 $\frac{X^2}{2}$		0.954		2.057	1.994
0(2)	0.347	0.366	0.277		0.971	0.971	1.961	1.956
0(3)	0.351 $\frac{X^2}{2}$	0.376			1.078		1.078	1.067
0(4)	0.465	0.465	0.320		1.083	1.868	1.601	1.601
0(5)			0.145	(0.013) $\frac{X^2}{2}$	0.887	0.917	1.949	2.187
0(6)			0.196	(0.010) $\frac{X^2}{2}$	0.898	0.932	2.026	2.187
0(7)				0.047	0.974 $\frac{X^2}{2}$		1.995	1.867
Σ	2.166	2.370	2.208	1.876	0.186	3.713	3.903	

vary in valence from +1(Li) to +4(Ti) and in size from ~ 0.535 (Al) to ~ 0.83 Å (Mn^{2+}), and having a variable anion substitution [at the O(3) site] than can involve O^{2-} , OH^- , F and Cl. There are at least three unique pseudo-octahedrally co-ordinated sites in each of the different amphibole structure-types. The significant differences in ligancy and local environment ensure considerable and complex cation ordering at these sites, a detailed knowledge of which is essential to the understanding of their crystal chemistry, physical properties and phase relations. The stereochemical details of this part of the structure are thus of primary importance in the interpretation of cation ordering patterns and frequently in the actual derivation of complete site-ordering patterns in the more complex chemical variants. Indeed, most recent work of Ungaretti (1980) and Ungaretti *et al.* (1981) has indicated that accurate chemical compositions (including $\text{Fe}^{3+}/\text{Fe}^{2+}$ ratios and even Li contents) and detailed patterns of ordering can be derived from high-quality X-ray data used in conjunction with detailed crystal-chemical analysis. Thus, the considerable effort expended on the characteri-

zation of ordering and stereochemistry in the octahedral strip in the past ten years is leading to increased understanding of chemical substitutions in amphiboles.

The $C2/m$ amphiboles

There are three unique sites with pseudo-octahedral co-ordination in this structure type, the M(1), M(2) and M(3) sites. The M(1) site has point-symmetry 2 and is co-ordinated by four oxygen atoms and two O(3) anions that may be OH^- , F^- , Cl^- or O^{2-} , with the O(3) anions arranged in a *cis* configuration. The M(1) octahedron shares five edges with the surrounding octahedra and one edge with the M(4) polyhedron. The M(2) site has point-symmetry 2 and is co-ordinated by six oxygen atoms; the M(2) octahedron shares three edges with neighboring octahedra and one edge with each of the two adjacent M(4) polyhedra. The M(3) site has point-symmetry $2/m$ and is co-ordinated by four oxygen atoms and two O(3) anions, the latter being arranged in a *trans* configuration. The M(3) octahedron shares six edges with the adjacent octahedra.

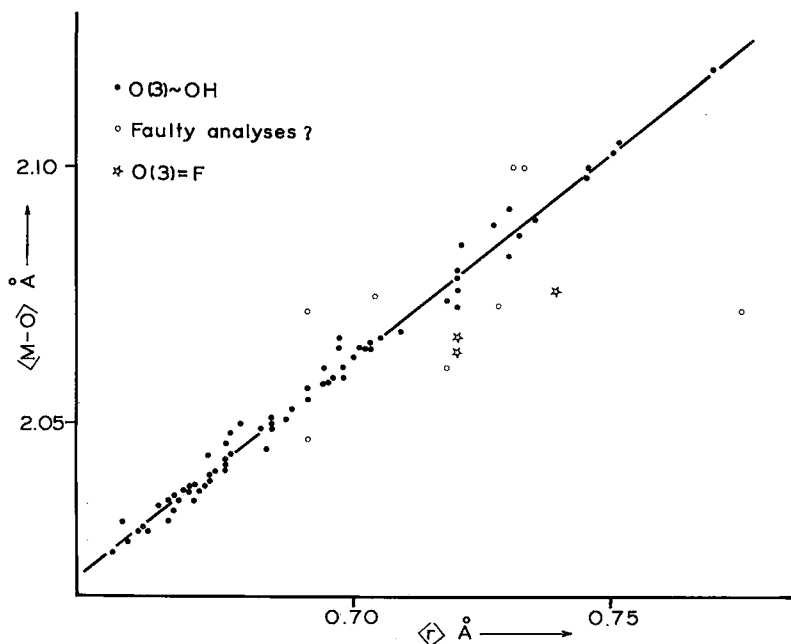


FIG. 42. Variation in grand $\langle \text{M-O} \rangle$ with mean ionic radius of the constituent cations for the $C2/m$ amphiboles. The regression line was calculated for hydroxy-amphiboles only, using data where the e.s.d. of the individual bond-lengths is less than 0.01 Å; data deviating significantly from the line were omitted from the regression analysis as the chemical composition of those specimens is suspect.

In many groups of isomorphous structures, the variation in mean bond-lengths of cation polyhedra may be related to the mean ionic radius of the cations occupying the sites. Thus the variations in the mean octahedral bond-lengths in garnet (Novak & Gibbs 1970, Hawthorne 1981c), olivine (Brown 1978) and pyroxene (Hawthorne & Grundy 1974, 1977c, Ribbe & Prunier 1977, Cameron & Papike 1981) are linear functions of the variation in radius of the constituent cation. Where this relationship is well characterized, it is extremely useful in deriving complete site-occupancies in cases where the results of a site-occupancy refinement do not give a unique solution, or to check out the consistency of the derived site-occupancies and the mean bond-lengths. The variation in grand mean bond-length as a function of grand mean ionic radius for the M(1), M(2) and M(3) sites in the $C2/m$ amphiboles is shown in Figure 42. A linear relationship is reasonably well developed, being described by the equation $\langle M-O \rangle = 1.527 + 0.764(17)\langle r \rangle$.

Some of the scatter in this figure is due to variation at the O(3) anion position, as the

data for the fluor-amphiboles indicate [$r(^{49}\text{F}) = 1.30 \text{ \AA}$; $r(^{49}\text{OH}) = 1.34 \text{ \AA}$]. However, some of the scatter seems to be due to bad or unrepresentative chemical analyses. For example, consider potassium arfvedsonite(66); the assigned site-populations (Appendix B3) indicate a mean radius of the constituent cations of 0.779 \AA that suggests a $\langle M-O \rangle$ of 2.122 \AA and is not compatible with the observed value of 2.098 \AA . Other questionable structures are also indicated in Figure 42, and discussed in detail in Appendix B3. Hence this relationship is a useful check on the compositional data for the crystal. Inclusion of the ionic radius of the O(3) anion into the above equation gives the relation $\langle M-O \rangle = 1.017 + 0.817(13)\langle r \rangle + 0.354(37)r_{\text{O}(3)}$. This may also be used to indicate the presence of F if one has confidence in the chemical data.

The grand $\langle M-O \rangle$ bond-length can also be calculated by summing the relevant cation and anion radii; a comparison of the values obtained with the observed data is given in Figure 43. There is a systematic deviation from the ideal hard-sphere model; the calculated values are

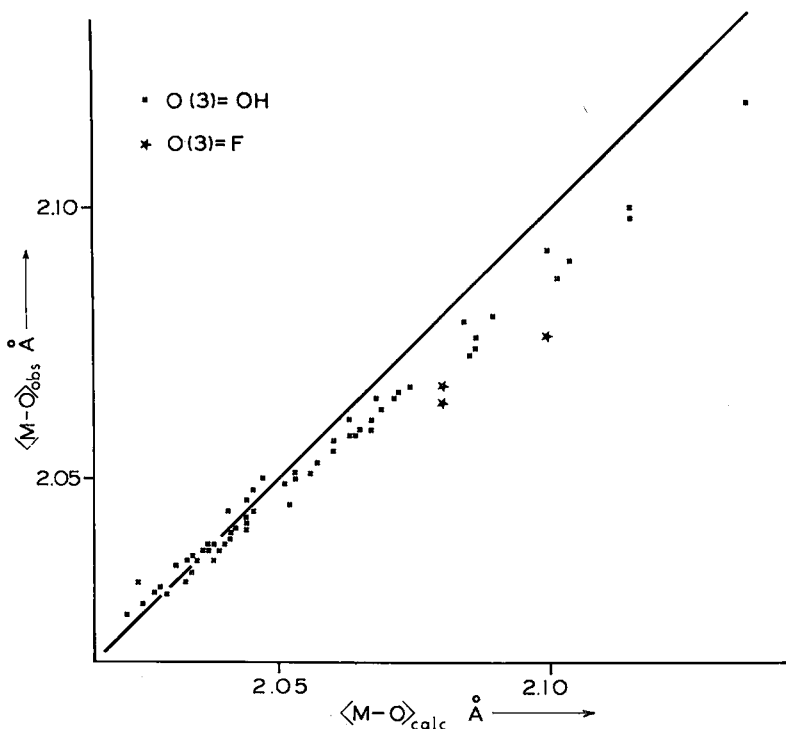


FIG. 43. Comparison of the grand $\langle M-O \rangle$ with the corresponding sum of the constituent cation and anion radii for the $C2/m$ amphiboles.

less than the ideal values at larger ionic radii, but the reason for this is not clear. Similar behavior is also exhibited by the pyroxenes and the garnets (Hawthorne 1981c). The fluor-amphiboles also deviate from the general trend of Figure 43; again, the reason is not clear.

In a refinement of the structure of magnesioriebeckite(3), Whittaker (1949) found that $\langle M(2)-O \rangle$ was significantly less than $\langle M(1)-O \rangle$ and $\langle M(3)-O \rangle$, indicating that Al was strongly ordered in this site and showing for the first time that the mean bond-lengths

in amphiboles were sensitive to cation site-occupancy. The same argument was later used by Papike & Clark (1968) to show a similar scheme of ordering in glaucophane. Robinson (1971) and Robinson *et al.* (1973) showed that $\langle M-O \rangle$ could be related to the mean ionic radius of the constituent cations in a series of four clin amphiboles and one fassaitic clinopyroxene, assuming that the Fe at the M(2) site in the hornblendes was Fe^{3+} . As the ligancy and local environment of the three octahedrally co-ordinated M sites differ considerably among

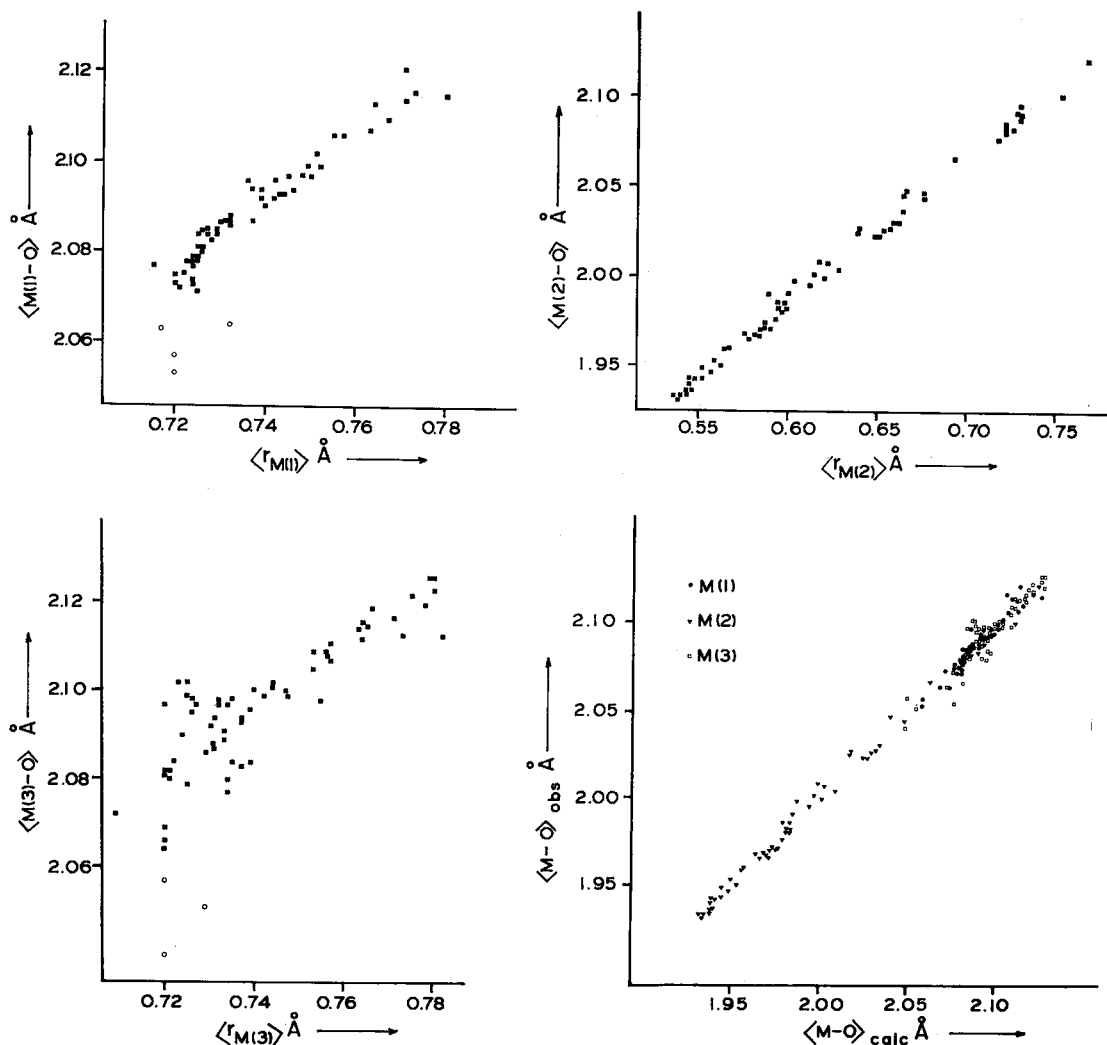


Fig. 44. Variation in individual $\langle M-O \rangle$ with mean ionic radius of the constituent cations for the $C2/m$ amphiboles (modified after Hawthorne 1978a). Also shown is a comparison of the observed mean bond-lengths at the octahedrally co-ordinated M sites with the corresponding values calculated from the regression equations of Table 27.

TABLE 27. REGRESSION ANALYSIS RESULTS FOR C2/m AMPHIBOLES

Dependent variable	Independent variable	c	m	R	σ	$ t $ ¹
<M(1)-O>	$r_{M(1)}$	0.877	0.82(3)	0.961	0.004	26.39
	$r_{O(3)}$		0.46(5)			8.50
<M(2)-O>	$r_{M(2)}$	1.488	0.827(8)	0.997	0.004	97.08
<M(3)-O>	$r_{M(3)}$	0.387	0.73(4)	0.925	0.007	16.34
	$r_{O(3)}$		0.87(9)			9.08
<M-O>	<r>	1.527	0.76(2)	0.983	0.004	43.68
<M-O>	<r>	1.017	0.82(1)	0.993	0.002	64.40
	$r_{O(3)}$		0.35(4)			9.46
<M(3)-O>	$r_{M(3)}$	0.773	0.69(4)	0.949	0.006	18.08
	$r_{O(3)}$		0.64(9)			7.06
	$r_{M(2)}$		-0.07(1)			5.43

¹ $|t|$ -values are calculated for the null hypothesis $H_0:m = 0.0$

themselves, it is best to examine such relationships separately for each site. This was originally done by Hawthorne (1978a) for a series of nineteen C2/m amphiboles, and has been extended here for the much larger data-set now available. Figure 44 shows the mean bond-length - ionic radius relationships for ~70 amphibole structures; less precise structures from Appendix B were omitted from this study. The relationship for the M(2) site is well developed and similar to those developed in previous studies. For the M(1) and M(3) sites, there is considerable scatter in these relationships; much of this stems from the variable occupancy of the O(3) site by OH⁻, F⁻, Cl⁻ and O²⁻. Inclusion of the mean ionic radius of the O(3) anion as an independent variable in a stepwise linear-regression analysis indicates that this factor contributes significantly to variations in the mean bond-lengths at the M(1) and M(3) sites; the results of this analysis are summarized in Table 27, and a comparison of the observed and calculated mean bond-lengths is given in Figure 44. As is apparent in Figure 44, significant scatter still exists, particularly in the relationship for the M(3) site. Hawthorne (1978a) has shown that octahedral distortion does not significantly contribute to mean bond-length variations in the clinoamphiboles and suggested that this scatter may result from incorrect assignment of site populations of such cations as Mn, Fe²⁺, Fe³⁺, Ti³⁺ and Ti⁴⁺ and such anions as OH, F, Cl and O²⁻. However, the results of Ungaretti *et al.* (1981) suggest some kind of inductive effect of other cations on the <M-O> bond-lengths. Figure 45 suggests that this is the case, <M(3)-O> being significantly affected by the mean size of the

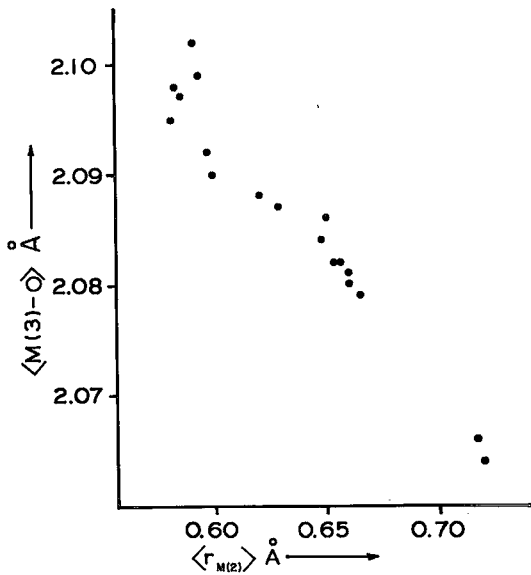


FIG. 45. Variation in <M(3)-O> as a function of the mean ionic radius of the constituent M(2) cations for values of $r_{M(2)}$ in the range 0.72-0.73 Å for the C2/m amphiboles.

constituent M(2) cation. Multiple regression analysis (Table 27) shows <M(3)-O> to be significantly affected by $\langle r \rangle_{M(2)}$. However, <M(1)-O> and <M(2)-O> are dependent only on their constituent cation and anion radii. Hawthorne (1979) has further examined the relationship for the M(2) site and concluded that either this relationship is nonlinear at small mean cation-radius values or the assigned site-populations for some amphiboles where $0.58 < r_{M(2)} < 0.68$ are incorrect; the latter is a distinct possibility, as the majority of the amphiboles in this class do not have experimentally determined Fe³⁺/Fe²⁺ ratios, and all Fe* (\equiv Fe²⁺ + Fe³⁺ + Mn) at M(2) was assumed to be Fe³⁺. The results of the current study indicate a linear relationship for the M(2) site, supporting the contention that some of the site occupancies are incorrect.

Hawthorne (1978a) has noted some unusual features in the mean bond-length - ionic radius relationships outlined above. They do not conform to a hard-sphere model ($\langle M-O \rangle = r_{\text{cation}} + r_{\text{anion}}$) particularly well. For the M(1) and M(3) octahedra, the slopes of the relationships are ~1.0, but the actual mean bond-lengths are ~0.02 Å less than values forecast from the sum of the relevant ionic radii. For the M(2) octahedron, the slope of the relationship (~0.74)

is less than the ideal value of 1.0. This suggests that the M(2) site is held open for small cations and compressed for large cations (Hawthorne 1978a). This is quite reasonable in terms of the rest of the octahedral strip. The *c* repeat of the M(1)–M(3)–M(1)–M(3)–M(1) chain has to be equal to the *c* repeat of the M(1)–M(2)–M(1)–M(2)–M(1) chain; consequently, when a great disparity exists between the sizes of the M(2) and M(3) cations, as is present if considerable Al occupies the M(2) site, the M(2) octahedron is held open by this requirement. As the size of the M(2) cation increases, this effect decreases as the size difference between the M(2) and M(3) cations decreases. If this is so, one might expect higher pressures to favor smaller cations at the M(2) site. This seems to be the case; prograde metamorphism leads to compositional changes in this direction, and amphiboles with high ^{vi}Al contents, such as tschermakite and glaucophane, are characteristic of high-pressure environments.

A somewhat different approach to mean bond-length variations in amphiboles has been taken by Litvin *et al.* (1972a) and Ungaretti *et al.* (1978), who proposed ideal mean bond-lengths for complete occupancy of an octahedral site by a specific cation. These values (Table 28) were subsequently used together with other structure-refinement results for

TABLE 28. IDEAL <M-O> DISTANCES (Å) FOR COMPLETE OCCUPANCY OF M(1,2,3) SITES BY A SINGLE CATION

	1		2		3		
Al	1.90	-	1.929	-	1.924	1.931	1.947
Fe ³⁺	2.03	-	2.031	-	2.014	2.022	2.027
Ti ⁴⁺	-	-	1.960	-	1.982	1.989	1.998
Ti ³⁺	-	-	-	-	2.035	2.043	2.045
Mg	2.07	2.078	2.078	2.083	2.075	2.084	2.082
Fe ²⁺	2.14	2.119	2.119	2.125	2.124	2.134	2.126
Mn ²⁺	-	-	-	-	2.165	2.175	2.163
Li	-	-	-	-	2.109	2.117	2.112

¹Litvin (1973); ²Ungaretti *et al.* (1981); ³calculated from the curves of Table 27 with O(3) = OH.

assignment of cation occupancy in amphiboles. A comparison of the values used by these authors with values derived from the regression relationships of Table 27 is shown in Table 28. There is fairly good agreement between the values, although significant differences do occur. These differences probably arise from the fact that the values of Ungaretti *et al.* (1978) were derived specifically from data on empty A-site alkali amphiboles, whereas the values derived here are derived from data on all amphiboles. There is almost certainly some variation in these values with amphibole type (*cf.* Fig. 45), and thus some difference is not unexpected.

TABLE 29. POLYHEDRON-DISTORTION PARAMETERS IN SELECTED C2/m AMPHIBOLES

	T(1)		T(2)		M(1)		M(2)		M(3)	
	Δ	σ ²	Δ	σ ²	Δ	σ ²	Δ	σ ²	Δ	σ ²
Grunerite(22)	0.29	0.8	0.78	15.8	2.25	36.0	2.79	43.2	0.11	60.9
Glaucophane(26)	0.05	0.6	1.88	17.4	0.21	69.5	15.77	35.0	0.34	85.0
Tremolite(30)	0.54	5.0	4.14	19.9	0.15	35.6	5.52	22.9	0.09	43.6
Fluor-richterite(34)	2.06	14.3	5.60	22.4	0.62	43.1	12.54	33.1	0.97	43.3
Fluor-tremolite(36)	0.38	6.2	3.45	19.3	0.01	46.9	5.76	21.9	1.03	47.9
Potassian pargasite(38)	0.59	6.6	1.42	19.1	1.25	50.5	5.98	24.3	0.01	75.7
Tirodite(41)	0.13	1.6	2.66	21.0	0.92	32.7	4.65	25.1	0.07	43.5
Magnesio-hornblende(42)	0.97	4.7	1.79	12.3	0.90	47.5	5.89	25.1	0.07	70.9
Hastingsite(44)	2.32	5.5	3.36	5.0	1.26	42.5	7.37	33.5	1.18	75.4
Ferro-tschermakite(54)	0.63	4.8	0.61	17.0	4.00	57.3	5.00	19.6	0.33	106.0
Potassian oxy-kaersutite(55)	0.29	5.8	1.16	18.9	14.35	47.9	7.06	31.2	0.05	56.8
Subsilicic titanian magnesian hastingsite(58)	0.31	4.6	0.78	17.1	3.59	65.0	6.87	23.4	0.08	107.9
Potassian ferri-taramite(59)	0.25	3.6	1.53	13.8	2.45	45.8	8.53	28.7	0.08	82.3
Sodian fluor- clinoholmquistite(62)	9.74	14.1	10.78	12.9	3.43	84.5	9.31	32.6	5.37	93.6
Potassium-arfvedsonite(67)	1.05	11.4	5.54	21.4	0.51	44.6	17.27	44.5	0.60	67.6
Fluor-riebeckite(68)	0.02	4.4	2.02	12.7	0.29	47.9	15.48	39.1	0.26	68.7
Ferro-glaucophane(69)	0.06	0.7	2.04	14.8	0.39	70.5	14.36	31.9	1.14	97.4

$$\Delta = \left[\sum_{i=1}^n [(x_i - x_m) / x_m]^2 / n \right] \times 10^4, \text{ where } x_i = \text{individual bond-length, } x_m = \text{mean bond-length,}$$

$$n = \text{number of bonds in coordination polyhedron; } \sigma^2 = \frac{n}{n-1} (\theta_i - \theta_m)^2 / (n-1), \text{ where } \theta_i = \text{indiv-}$$

idual bond-angle, θ_m = ideal bond-angle, n = number of bond angles in coordination polyhedron.

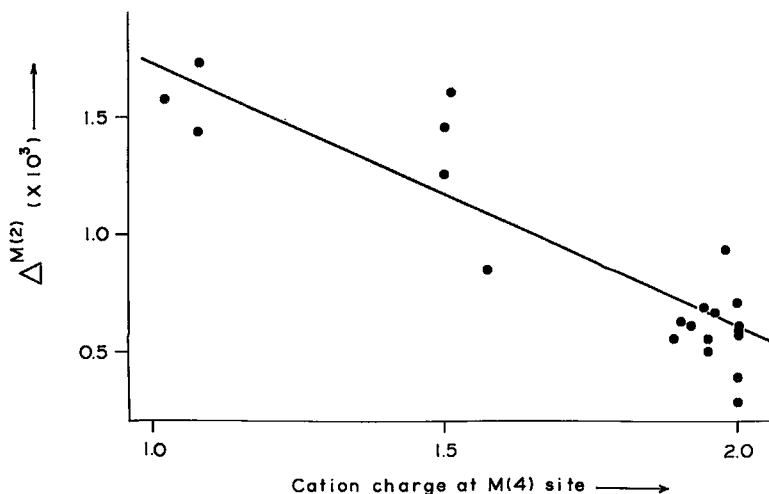


FIG. 46. Variation in polyhedral distortion Δ of the M(2) polyhedron as a function of the mean formal cation charge at the M(4) site in the $C2/m$ amphiboles [after Hawthorne (1976)].

The recent development of bond-valence-bond-length relationships (Baur 1970, 1971, Donnay & Allmann 1970, Brown & Shannon 1973, Brown & Wu 1976, Pyatenko 1973, Ferguson 1974) has indicated that bond-valence requirements are a major factor in controlling bond-length variations in inorganic structures. Amphiboles exhibit considerable deviations from Pauling's second rule (Pauling 1960) for a formal bond-strength model, and thus bond-valence requirements should have an extremely strong effect on bond-length variations in amphiboles. Tables 19 and 26 show empirical bond-valence tables for selected amphiboles, in which it can be seen that the bond-length variations observed tend to minimize the deviations from ideality in the bond-valence sums around the anions. As we saw when examining the tetrahedral double-chain, this is particularly significant with respect to cations co-ordinating the O(4) anion, all of which show extremely short bonds to O(4). In order to maintain mean bond-lengths in accord with the size of the constituent cations, there is a concomitant lengthening of the other bonds to these cations, resulting in extremely distorted cation-sites. This is evident from Table 29, which lists some distortional parameters for the cation polyhedra in selected amphibole structures. Also in accord with this argument is the correlation between the dispersion of the M(2)-O bond-lengths and the mean charge of the M(4) cations (Fig. 46).

Hawthorne (1978a) has also examined bond-length variations in the octahedra of the

clinoamphiboles using the methods of Baur (1970, 1971). Sample calculations for tremolite (30), glaucophane(26) and pargasite(38) are shown in Table 30. For *a priori* prediction of distances, the calculated bond-lengths at the M(1) and M(3) sites are generally larger than the observed values, in agreement with the fact that the observed mean bond-lengths are significantly less than the sum of the constituent ionic radii. Conversely, the calculated bond-lengths for the M(2) octahedron are small and the amount of deviation from the observed values appears to be correlated with the mean ionic radius of the constituent M(2) cations. This behavior is directly analogous to the mean bond-length - mean constituent-cation radius relationships outlined earlier. A more accurate prediction of bond lengths can be made if Baur's relationships are used to forecast the deviation of individual bond-lengths from a mean value predicted from the regression relationships of Table 27. As indicated in Table 30, this does produce an improvement over the *a priori* values, but discrepancies between observed and calculated values are still large. This is not surprising, as bond-valence requirements do not provide sufficient constraints to exactly define the structure. Additional features such as cation-cation repulsion and intermodule linkage requirements will also have an effect on bond-length variations, an effect that is not recognized in the bond-valence models.

It has been suggested (Pauling 1960) that

TABLE 30. BOND LENGTHS FOR SELECTED AMPHIBOLES CALCULATED BY THE METHOD OF BAUR (1970, 1971)

	p_x	Δp_x	d_{calc}^1	d_{calc}^2	d_{obs}	Δd^1	Δd^2
Tremolite(30)							
M(1)-O(1)	2.00	+0.027	2.090	2.078	2.064	-0.026	-0.014
M(1)-O(2)	1.92	-0.053	2.080	2.069	2.078	-0.002	+0.009
M(1)-O(3)	2.00	+0.027	2.090	2.078	2.083	+0.007	+0.005
Mean	1.973		2.087	2.075	2.075		
M(2)-O(1)	2.00	+0.167	2.090	2.097	2.133	+0.043	+0.036
M(2)-O(2)	1.92	+0.087	2.080	2.087	2.083	+0.003	-0.004
M(2)-O(4)	1.58	-0.253	2.040	2.047	2.014	-0.026	-0.033
Mean	1.833		2.070	2.077	2.077		
M(3)-O(1)	2.00	0.000	2.090	2.066	2.070	-0.020	+0.004
M(3)-O(3)	2.00	0.000	2.090	2.066	2.057	-0.033	-0.009
Mean	2.00		2.090	2.066	2.066		
Glaucophane(26)							
M(1)-O(1)	2.17	+0.127	2.126	2.106	2.078	-0.047	-0.028
M(1)-O(2)	1.96	-0.083	2.095	2.075	2.082	-0.013	+0.007
M(1)-O(3)	2.00	-0.043	2.101	2.081	2.100	-0.001	+0.019
Mean	2.043		2.107	2.087	2.087		
M(2)-O(1)	2.17	+0.250	1.959	2.003	2.038	+0.079	+0.035
M(2)-O(2)	1.96	+0.040	1.909	1.953	1.943	+0.034	-0.010
M(2)-O(4)	1.63	-0.290	1.830	1.874	1.849	+0.019	-0.025
Mean	1.920		1.899	1.943	1.943		
M(3)-O(1)	2.17	+0.057	2.139	2.104	2.103	-0.036	-0.001
M(3)-O(3)	2.00	-0.113	2.110	2.075	2.077	-0.033	+0.002
Mean	2.113		2.129	2.094	2.094		
Pargasite(38)							
M(1)-O(1)	1.98	-0.013	2.103	2.086	2.056	-0.047	-0.030
M(1)-O(2)	2.00	+0.007	2.106	2.089	2.111	+0.005	+0.022
M(1)-O(3)	2.00	+0.007	2.106	2.089	2.093	-0.009	+0.008
Mean	1.993		2.105	2.088	2.088		
M(2)-O(1)	1.98	+ .100	2.013	2.053	2.069	+0.056	+0.016
M(2)-O(2)	2.00	+ .120	2.017	2.057	2.074	+0.057	+0.017
M(2)-O(4)	1.66	- .220	1.957	1.997	1.966	+0.009	-0.031
Mean	1.880		1.996	2.036	2.036		
M(3)-O(1)	1.98	-0.007	2.103	2.076	2.076	-0.027	0.000
M(3)-O(3)	2.00	+0.013	2.106	2.079	2.080	-0.026	+0.001
Mean	1.987		2.104	2.077	2.077		

¹calculated from the relationship $d=a+bp_x$ (Baur 1970) where d is the predicted bond length, p_x is the sum of the formal bond strengths received by the anion, and a and b are empirically derived constants

²calculated from the relationship $d=<d_{mean}>+\Delta bp_x$, where Δp_x is the bond strength sum deviation from the mean value received by the anions in a coordination polyhedron

cation-cation repulsive interactions are much stronger than anion-anion repulsive interactions and that, as a result, edges shared between polyhedra are shorter and subtend smaller angles at the cation than unshared edges. In the octahedral strip of the clinoamphibole structure, the M(1), M(2) and M(3) octahedra share six, five and six edges, respectively, with adjacent cation polyhedra, suggesting that cation-cation repulsion should play an important role in bond-angle distortion. As indicated in Figure 47, this appears to be the case. For the M(1) and M(3) octahedra, the separation of the edges and angles into two populations corresponding to shared and unshared elements, together with the marked linear correlations exhibited, suggest that cation-cation repulsion is of prime importance. For the M(2) octahedron, although there is a tendency for the data to separate out into two populations corresponding to shared and unshared elements, considerable overlap occurs and the linear correlation is far less marked than for the M(1) and M(3) octahedra. Hawthorne (1978a) has proposed that a considerable amount of the angular distortion of the M(2) octahedron is a direct result of the O(4) bond-valence requirements. To assess the magnitude of this effect, the bond angles were calculated for a holosymmetric octahedron with the observed bond-lengths of tremolite(30), fluor-richterite(34) and fluor-tremolite(36). The results are given in Table 31, where they are compared with the observed values. It is apparent that the anion bond-valence requirements have a considerable effect on the bond-

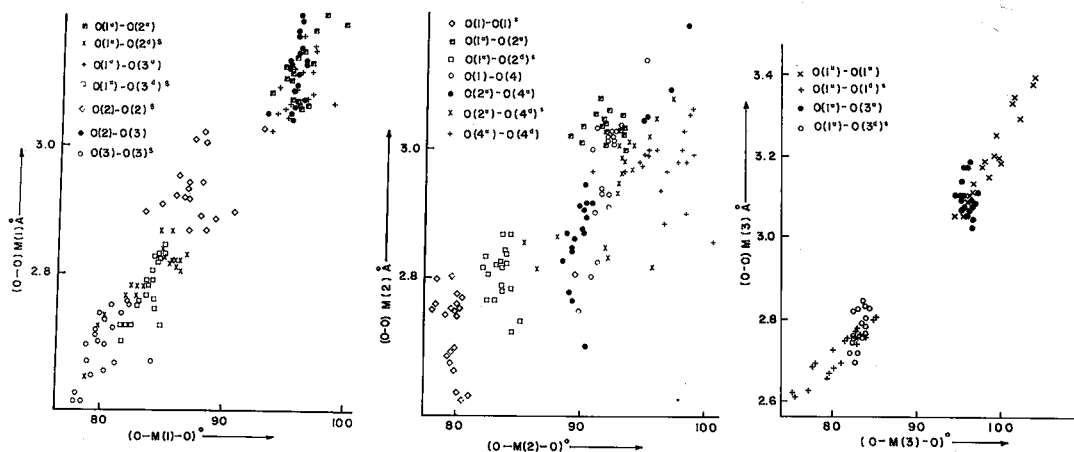


FIG. 47. Variation in length of the octahedral edges with the corresponding angles subtended at the cation for the octahedrally co-ordinated M sites in a variety of $C2/m$ amphiboles.

TABLE 31. CALCULATED O-M(2)-O ANGLES($^{\circ}$) IN AMPHIBOLES WITH M(1)=M(2)=M(3) \sim Mg*

	Tremolite(30)		Fluor-tremolite(36)		Fluor-richterite(34)		Antho-phyllite[23]		Proto-amphibole[20]	
	obs.	calc.	obs.	calc.	obs.	calc.	obs.	calc.	obs.	calc.
0(1)-M(2)-0(1)	80.0	86.8	80.0	86.5	79.7	84.6	80.4	86.9	79.6	84.7
0(1 ^u)-M(2)-0(2 ^u)	92.1	87.9 88.1	91.9	87.8 88.3	90.2	86.4 87.7	92.5	88.4 88.4	91.4	87.7 87.1
0(1 ^u)-M(2)-0(2 ^d)	83.7		83.7		82.6		84.3		83.5	
0(1)-M(2)-0(4)	92.8	89.9	92.6	89.7	91.0	88.9	93.1	89.6	90.9	89.5
0(2 ^u)-M(2)-0(4 ^u)	90.3	91.9 91.4	90.5	91.9 91.6	90.5	93.0 92.5	97.0	91.5 91.3	97.5	92.0 92.3
0(2 ^u)-M(2)-0(4 ^d)	93.4		93.3		95.6		86.0		86.4	
0(4)-M(2)-0(4)	95.0	93.4	95.5	93.2	99.1	94.0	93.4	92.8	98.5	95.2

*angles calculated for a holosymmetric octahedron with the observed M-O bond lengths.

angle distortions of the M(2) site. This is presumably the reason why the correlation for the M(2) site exhibited in Figure 47 is less than for the M(1) and M(3) sites, where the anion bond-valence requirements are not as extreme.

Fleet (1974) has examined polyhedral distortions in three amphiboles in terms of cation-cation repulsion across shared polyhedral edges. He noted that the M-M distances parallel to the Y axis [M(1)-M(1), M(1)-M(4) and M(2)-M(3)] are stretched the most (Cameron & Gibbs 1973) and suggested that this must reflect the relative rigidity of the tetrahedral element parallel to the Z axis. This seems to be most unlikely; much more important is the fact that the tetrahedra will tilt relative to their mirror equivalents to encompass expansion in the Y direction. Hawthorne (1978a) has also examined some of the factors that can affect elements shared between adjacent octahedra. There is considerable variation in the size of the octahedra in the clinoamphiboles with variation in cation occupancy. As polyhedral elements are shared between octahedra of disparate size, shared elements must adjust accordingly. Prominent in this respect is the mean size of the cations occupying the M(2) site; the variance in the octahedral angle at both the M(1) and M(3) sites is negatively correlated with mean ionic radius of the constituent M(2) cations (Fig. 48). Thus the mean ionic radius of the constituent M(2) cation could have a significant effect on the CFSE of transition-metal cations at the M(1) and M(3) sites, and significantly affect cation ordering patterns.

The $P2_1/m$ amphiboles

There are three unique sites with pseudo-octahedral co-ordination in this structure-type, the M(1), M(2) and M(3) sites. Both the octahedra

and the way they link together are similar to the corresponding octahedra in the $C2/m$ amphiboles. However, the point-symmetry of the M(1), M(2) and M(3) sites is 1, 1 and m , respectively. Our understanding of this structure-type suggests that it should be of magnesio-cummingtonite composition. In agreement with this, nearly all $P2_1/m$ amphiboles reported are restricted to this compositional range (Ross *et al.* 1968a, Kisch 1969, Rice *et al.* 1974, Yakovleva *et al.* 1978). This being the case, the octahedral sites will show virtually complete occupancy by Mg, and the only octahedral bond-length variations expected in this structure-type will be due to inductive effects of the M(4) cation(s). Thus the octahedral strip element of tirodite $P2_1/m(27)$ should be fairly representative of all compositional variations in this structure-type.

In tirodite $P2_1/m(27)$, the octahedral sites are completely occupied by Mg, and the mean bond-lengths are not significantly different from those forecast from the curves of Table 27 for the $C2/m$ amphiboles. Table 32 compares the individual bond-lengths in tremolite(30) with the corresponding mean values in tirodite $P2_1/m(27)$. The only significant difference is in the M(1)-O(2) bond, which is 0.030(4) Å longer in the $P2_1/m$ structure. This may be interpreted as an inductive effect due to the change in the M(4) cation. The bonding radius of (Mg, Fe) is much smaller than that of Ca, and thus the interaction between the M(4) cation(s) and the chain-bridging anions will be much weaker in Fe-Mg-Mn amphiboles. In order to satisfy the bond-valence requirements of the M(4) cation(s), the bonding to the non-bridging anions O(2) and O(4) will have to be stronger in tirodite $P2_1/m(27)$ than in tremolite. In order to accommodate this, the M(1)-O(2) bonds are longer in tirodite $P2_1/m(27)$ than in

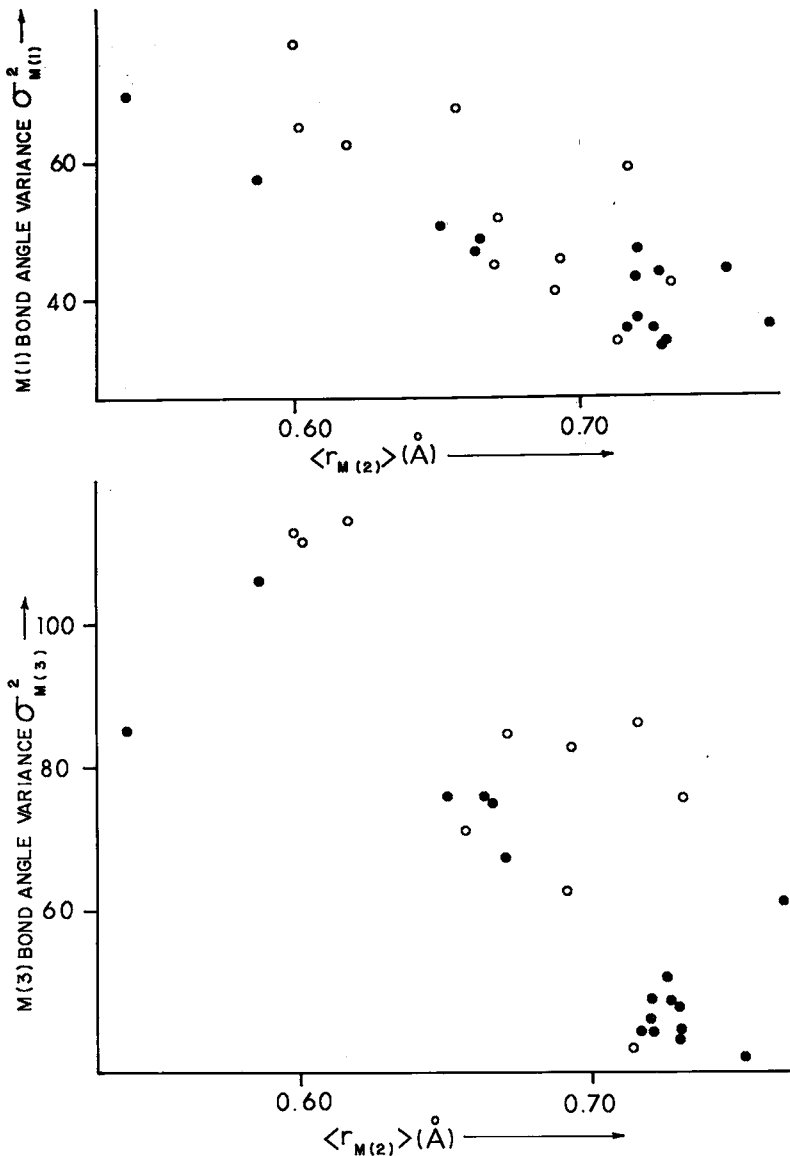


FIG. 48. Variation of the variance σ^2 in the octahedral angle for M(1) and M(3) with the mean ionic radius of the M(2) cations for $C2/m$ amphiboles (after Hawthorne 1978a). Open circles denote additional data from less precise structures.

tremolite(30). Examination of the differences between the M-O(A) and M-O(B) bonds (Table 32) shows that the only significant differences occur for the O(2A) and O(2B) anions. This reinforces the above conclusion that the inductive effect of the M(4) cation affects the octahedral strip through the O(2A) and O(2B) anions.

All elements shared between adjacent octahedra are greater than all unshared elements, indicating the influence of cation-cation repulsion. In addition, this amphibole agrees with the correlations developed for the $C2/m$ amphiboles (Hawthorne 1978a), indicating that packing considerations and bond-valence requirements significantly affect interbond angles

TABLE 32. COMPARISON OF M-O BOND LENGTHS IN TIRODITE $P2_1/m(27)$ AND TREMOLITE(30)

	tirodite $P2_1/m(27)$ (averaged)	tremolite(30)	diff.
M(1)-0(1)	2.058(5) ⁰ Å	2.064(2) ⁰ Å	0.006(6) ⁰ Å
M(1)-0(2)	2.108(4)	2.078(2)	0.030(4)
M(1)-0(3)	2.076(4)	2.083(2)	0.007(4)
M(2)-0(1)	2.139(4)	2.133(2)	0.006(4)
M(2)-0(2)	2.081(5)	2.083(2)	0.002(6)
M(2)-0(4)	2.014(5)	2.014(2)	0.000(6)
M(3)-0(1)	2.080(5)	2.070(2)	0.010(6)
M(3)-0(3)	2.060(8)	2.057(3)	0.003(9)

and the amount of structural relaxation due to cation-cation repulsion.

The $P2/a$ amphiboles

There are five unique sites with pseudo-octahedral co-ordination in this structure-type, the M(1)A, M(1)B, M(2)A, M(2)B and M(3) sites. The M(1)A and M(1)B sites have point-symmetry 2 and are co-ordinated by four oxygen atoms and two O(3) anions that are OH in the only representative of this structure-type found (Moore 1968a, b, 1969); the O(3) anions are arranged in a *cis* configuration. The M(2)A and M(2)B sites have point-symmetry 2 and are co-ordinated by six oxygen atoms. The M(3) site has point-symmetry 2 and is co-ordinated by four oxygen atoms and two O(3) anions arranged in a *trans* configuration. The edge-sharing characteristics of these octahedra are similar to those found in the $C2/m$ amphibole structure.

Joessmithite (Moore 1969) is the only amphibole of this structure-type that is known. Polyhedral distortions, aside from effects of local electroneutrality, result largely from cation-cation repulsion effects. Shared edges between octahedra are the shortest distances for each of the polyhedra, and subtend the smallest angles at the central cation.

The $Pnma$ amphiboles

There are four unique sites with pseudo-octahedral co-ordination in this structure-type, the M1, M2, M3 and M4 sites. However, the M4 site will not be regarded as part of the octahedral strip, and discussion of it will be deferred until later. The M1 site has point-symmetry 1 and is co-ordinated by four oxygen

atoms and two O3 anions that may be OH⁻, F⁻, or O²⁻, with the O3 anions arranged in a *cis* configuration. The M1 octahedron shares five edges with the surrounding octahedra of the strip and one edge with the M4 octahedron. The M2 site has point-symmetry 1 and is co-ordinated by six oxygen atoms; the M2 octahedron shares three edges with neighboring octahedra of the strip and two edges with the adjacent M4 octahedra. The M3 site has point-symmetry *m* and is co-ordinated by four oxygen atoms and two O3 anions, the latter being arranged in a *trans* configuration. The M3 octahedron shares six edges with the adjacent octahedra of the strip. For the octahedral strip derived from the cations of the asymmetric unit, anions with $x > 0$ are B-type anions whereas anions with $x < 0$ are A-type anions (note correspondence with *u-d* nomenclature of the monoclinic amphiboles).

The relationship between grand mean octahedral bond-length and grand mean constituent-cation radius for the M1, M2 and M3 sites is shown in Figure 49. The values for anthophyllite[23], holmquistite[31] and gedrite[32] are linear, forming a trend that is approximately parallel to the corresponding relationship for the $C2/m$ amphiboles. However, the value for gedrite[33] deviates by almost 0.01 Å in $\langle r \rangle$, indicating that the bulk chemistry of the sample is not compatible with the structure-refinement results. This is discussed in more detail in Appendix B3. Linear regression on the remaining three values gives the following relationship: $\langle M-O \rangle = 1.484 + 0.823 \langle r \rangle$ $R = 0.99$.

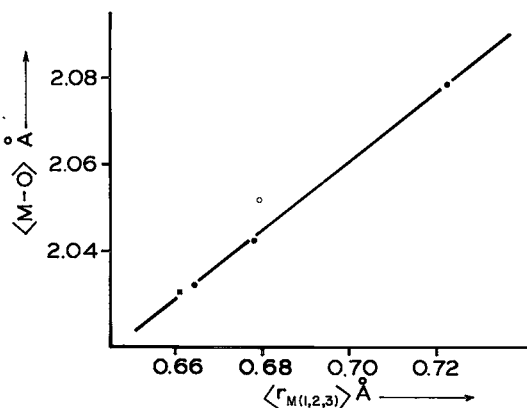


FIG. 49. Variation in grand $\langle M-O \rangle$ with mean ionic radius of the constituent cations for the $Pnma$ amphiboles; gedrite[33], denoted by the open circle, was omitted from the regression analysis.

The utility of this relationship is apparent immediately in its indication of the unsatisfactory nature of the chemical analysis of gedrite[33].

Papike & Ross (1970) and Irusteta & Whittaker (1975) noted that $\langle M2-O \rangle$ in gedrite[32] and [33] and holmquistite[31], respectively, are smaller than $\langle M1-O \rangle$ and $\langle M3-O \rangle$ due to occupancy of M2 by considerable amounts of Al. However, a more systematic examination of mean octahedral bond-length variation in the orthorhombic amphiboles has not been given until now. The relevant data are summarized in Table 33 and in Figure 50, where the possible variation in constituent-cation radius is shown. Consider first the relationship for the M2 site. The minimum value for holmquistite[31], the maximum value for gedrite[33] and anthophyllite[23] are collinear. The values for gedrite[32] assigned from the site occupancy of Papike & Ross (1970) straddle this trend. For the M1 and M3 sites, the values for anthophyllite are well defined; as a starting approximation, the curves were assumed to pass through the values for anthophyllite with a slope of 1.0. The values for each site consistent with the overall stoichiometry of each amphibole are marked on each of the graphs (Fig. 50). There seems to be satisfactory agreement, except for gedrite[33], which shows a low $\langle r \rangle$ at the M3 site. Note that these curves indicate that the crystal of gedrite[32] used in the structure refinement has Fe^{3+} at the M(3) site. The paucity of the data does not really warrant linear regression analysis at the present time, particularly as some of the site populations are not that well characterized. However, the equations of the curves derived in Figure 50 are: $\langle M(1)-O \rangle = 1.362 + \langle r_{M(1)} \rangle$, $\langle M(2)-O \rangle = 1.513 + 0.782 \langle r_{M(2)} \rangle$ and $\langle M(3)-O \rangle = 1.348 + \langle r_{M(3)} \rangle$.

Note that these relationships are similar to those of the $C2/m$ amphiboles in that the observed mean bond-lengths are $\sim 0.02 \text{ \AA}$ less than the sum of the constituent ionic radii, and the slope of the bond length-ionic radius relationship for the M2 site is significantly less than the ideal value of 1.0.

The $Pnma$ orthoamphiboles show considerable deviations from Pauling's second rule (Pauling 1960) for a formal bond-strength model, and thus bond-strength requirements should have an extremely strong effect on bond-length variations in orthoamphiboles. Table 22 shows bond-valence tables together with the formal bond-strength sums around the anions. Inspec-

TABLE 33. $\langle M-O \rangle$ DISTANCES AND RANGE OF POSSIBLE CONSTITUENT CATION RADII CONSONANT WITH X-RAY SITE POPULATIONS AND CELL CONTENTS FOR THE $Pnma$ AMPHIBOLES

		$\langle M-O \rangle^0$	$\langle r \rangle_{\min}^0$	$\langle r \rangle_{\max}^0$
Anthophyllite[23]	M 1	2.084(1)		0.722
	M 2	2.076(1)		0.721
	M 3	2.070(2)		0.722
Holmquistite[31]	M 1	2.100(3)	0.737	0.744
	M 2	1.932(4)	0.538	0.548
	M 3	2.095(4)	0.740	0.754
Gedrite[32]	M 1	2.091(4)	0.711	0.727
	M 2	1.986(4)	0.604	0.605
	M 3	2.057(4)	0.713	0.726
Gedrite[33]	M 1	2.101(3)	0.730	0.740
	M 2	1.979(3)	0.585	0.594
	M 3	2.097(4)	0.725	0.743

tion of this table shows that the bond-length variations observed tend to minimize the deviations from ideality in the bond-valence sums around the anions. As with the $C2/m$ amphiboles, this accounts for the cations showing short bonds to the O4A and O4B anions. In addition, where M4 is occupied by a monovalent cation (Li^+), the M2 octahedron is much more distorted than where M4 is occupied by a divalent cation. Examination of the orthorhombic amphiboles using the scheme of Baur (1970, 1971) is shown in Table 34. The results are very similar to those for the $C2/m$ amphiboles. Bond lengths calculated for the M1 and M3 octahedra are generally larger than the observed values, whereas the deviation between the observed and calculated bond-lengths for the M2 octahedron is correlated with the mean ionic radius of the constituent M2 cation.

Polyhedral distortion seems to be dominantly due to cation-cation repulsion, locally modified by factors specific to the amphibole structure. The distortion of the three octahedra in terms of shared and unshared elements is examined in Figure 51; the results are similar to those of the $C2/m$ amphiboles. For the M1 and M3 octahedra, the data separate out into two populations corresponding to shared and unshared elements. For the M2 octahedron, there is some overlap between the two populations, and the linear correlation is far less marked than for the M1 and M3 octahedra. The arguments put forward by Hawthorne (1978a) for the $C2/m$ amphiboles should be directly applicable to the $Pnma$ amphiboles. Thus the angular distortion of the M1 and M3 octahedron should be a function of the mean ionic radius of the constituent M2 cations; Figure 52 shows this to be the case. Similarly, the O4A and O4B bond-valence requirements should

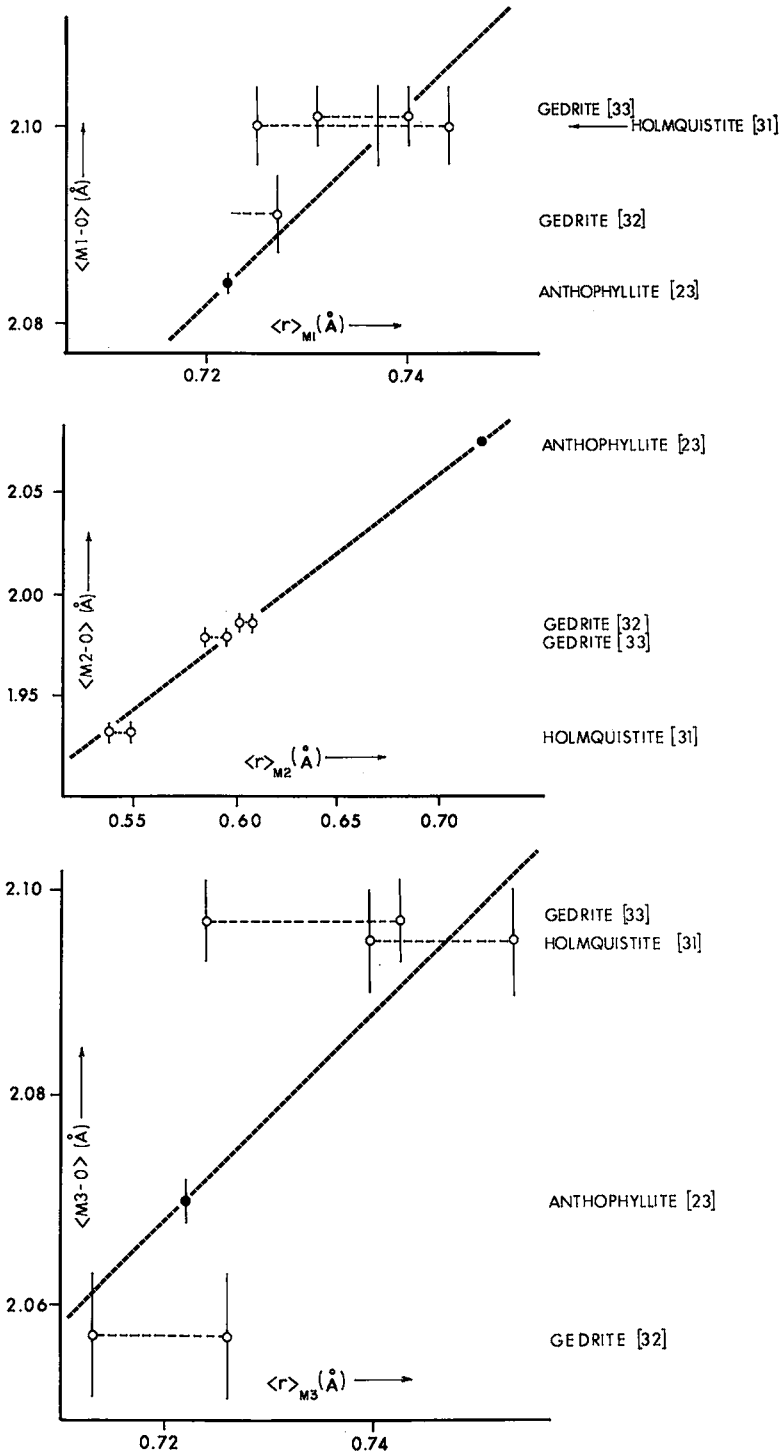


FIG. 50. Variation in individual $\langle M-O \rangle$ with mean ionic radius of the constituent cations for the $Pnma$ amphiboles; the possible ranges in mean ionic radius of the constituent at each site consonant with the diffraction

considerably affect the angular distortion of the M2 octahedron, as seems to be the case for anthophyllite[23], as shown in Table 31.

The Pnmn amphiboles

There are three unique sites with pseudo-octahedral co-ordination in this structure-type, the M1, M2 and M3 sites; these are similar to the analogous sites in the C2/m amphiboles. It should be noted that the M4 site is also probably [6]-co-ordinate, but this polyhedron will be considered in the section on the M(4)

Gedrit[32]

	M4 = [6] Coordinate						obs.
	p _x	d ¹	d ²				
M1-01A	2.102	2.113	2.094	-	-	-	2.067(9)
M1-02A	2.165	2.122	2.103	-	-	-	2.130(9)
M1-03A	2.000	2.098	2.079	-	-	-	2.078(9)
M1-01B	2.095	2.112	2.093	-	-	-	2.054(10)
M1-02B	2.133	2.117	2.098	-	-	-	2.158(8)
M1-03B	2.000	2.098	2.079	-	-	-	2.061(8)
Mean	2.083	2.110	2.091	-	-	-	2.091
M2-01A	2.102	1.998	2.002	-	-	-	2.028(8)
M2-02A	2.165	2.010	2.014	-	-	-	1.985(10)
M2-04A	1.832	1.945	1.949	-	-	-	1.924(9)
M2-01B	2.095	1.997	2.001	-	-	-	2.005(9)
M2-02B	2.133	2.004	2.008	-	-	-	2.021(8)
M2-04B	1.800	1.939	1.943	-	-	-	1.951(8)
Mean	2.021	1.982	1.986	-	-	-	1.986
M3-01A	2.102	2.111	2.062	-	-	-	2.055(8)
M3-03A	2.000	2.097	2.048	-	-	-	2.017(15)
M3-01B	2.095	2.110	2.061	-	-	-	2.097(9)
M3-03B	2.000	2.097	2.048	-	-	-	2.023(13)
Mean	2.066	2.106	2.057	-	-	-	2.057

TABLE 34. BOND LENGTHS (Å) FOR SELECTED Pnmn AMPHIBOLES CALCULATED BY THE METHOD OF BAUR (1970, 1971)

Anthophyllite[23]

	M4 = [5] Coordinate			M4 = [7] Coordinate			obs.
	p _x	d ¹	d ²	p _x	d ¹	d ²	
M1-01A	1.995	2.091	2.081	1.995	2.091	2.086	2.062(3)
M1-02A	2.061	2.100	2.089	1.947	2.086	2.080	2.112(3)
M1-03A	2.000	2.092	2.082	2.000	2.092	2.086	2.082(3)
M1-01B	1.995	2.091	2.081	1.995	2.091	2.086	2.053(4)
M1-02B	2.064	2.101	2.090	1.950	2.086	2.080	2.133(3)
M1-03B	2.000	2.092	2.082	2.000	2.092	2.086	2.063(3)
Mean	2.019	2.094	2.084	1.981	2.090	2.084	2.084
M2-01A	1.995	2.091	2.084	1.995	2.091	2.088	2.138(3)
M2-02A	2.061	2.099	2.092	1.947	2.086	2.082	2.067(3)
M2-04A	1.728	2.059	2.051	1.614	2.044	2.040	2.010(3)
M2-01B	1.995	2.091	2.084	1.995	2.091	2.088	2.121(3)
M2-02B	2.064	2.100	2.093	1.950	2.086	2.082	2.082(3)
M2-04B	1.731	2.060	2.051	1.617	2.044	2.041	2.037(3)
Mean	1.929	2.083	2.076	1.853	2.074	2.076	2.076
M3-01A	1.995	2.091	2.070	1.995	2.091	2.070	2.075(3)
M3-03A	2.000	2.092	2.070	2.000	2.092	2.070	2.055(5)
M3-01B	1.995	2.091	2.070	1.995	2.091	2.070	2.079(3)
M3-03B	2.000	2.092	2.070	2.000	2.092	2.070	2.059(5)
Mean	1.997	2.091	2.070	1.997	2.091	2.070	2.070

Holmquistite[31]

	M4 = [5] Coordinate			M4 = [7] Coordinate			obs.
	p _x	d ¹	d ²	p _x	d ¹	d ²	
M1-01A	2.156	2.148	2.118	2.156	2.148	2.122	2.086(6)
M1-02A	2.033	2.124	2.094	1.976	2.113	2.087	2.123(9)
M1-03A	2.000	2.118	2.088	2.000	2.118	2.092	2.095(9)
M1-01B	2.156	2.148	2.118	2.156	2.148	2.122	2.079(9)
M1-02B	2.033	2.124	2.094	1.976	2.113	2.087	2.123(9)
M1-03B	2.000	2.118	2.088	2.000	2.118	2.092	2.095(8)
Mean	2.063	2.130	2.100	2.044	2.126	2.100	2.100
M2-01A	2.156	1.954	1.978	2.156	1.954	1.987	2.013(9)
M2-02A	2.033	1.925	1.949	1.976	1.911	1.944	1.941(10)
M2-04A	1.700	1.845	1.869	1.643	1.832	1.865	1.828(9)
M2-01B	2.156	1.954	1.978	2.156	1.954	1.987	2.029(9)
M2-02B	2.033	1.925	1.949	1.976	1.911	1.944	1.938(10)
M2-04B	1.700	1.845	1.869	1.643	1.832	1.865	1.841(10)
Mean	1.963	1.908	1.932	1.925	1.899	1.932	1.932
M3-01A	2.156	2.164	2.103	2.156	2.164	2.103	2.103(9)
M3-03A	2.000	2.130	2.069	2.000	2.130	2.069	2.077(14)
M3-01B	2.156	2.164	2.103	2.156	2.164	2.103	2.109(9)
M3-03B	2.000	2.130	2.069	2.000	2.130	2.069	2.070(13)
Mean	2.104	2.153	2.095	2.104	2.153	2.095	2.095

¹calculated from the relationship $d = a + bp_x$, where d is the predicted bond length, p_x is the sum of the formal bond-strengths received by the anion, and a and b are empirically derived constants (Baur 1970)

²calculated from the relationship $d = <d_{obs}> + b\Delta p_x$, where Δp_x is the formal bond-strength minus the mean anion bond-strength sum in a coordination polyhedron

site. Only one example of this structure-type has been reported (Gibbs 1962, 1969, Gibbs *et al.* 1960); this was called "protoamphibole" as it appears to bear the same relationship to tremolite and anthophyllite as protoenstatite (Smith 1969) does to diopside and enstatite. In protoamphibole, the M1, M2 and M3 sites are completely occupied by Mg. Table 35 compares the octahedral bond-lengths in protoamphibole[20] with those in tremolite(30), fluor-richterite(34) and fluor-tremolite(36). The <M1-O> in protoamphibole[20] is significantly greater than the corresponding distances in fluor-richterite(34) and fluor-tremolite(36), being almost as large as <M1-O> in tremolite(30). However, <M3-O> for protoamphibole[20] is intermediate between the values for fluor-richterite(34) and fluor-tremolite(36), and it is difficult to explain the large <M1-O> distance; <M(2)-O> is statistically identical in all three fluor-amphibole structures and is equal to the corresponding distance in tremolite(30).

The stereochemistry of the octahedral strip is similar to that of the natural amphiboles. Inspection of the empirical bond-valence table for protoamphibole[22] (Table 23) shows that

data and chemical analysis are shown (open circles). The relationship shown in each graph was derived to obtain the best fit for all three sites, together with the constraint that these relationships should be fairly similar to the analogous ones for the C2/m amphiboles.

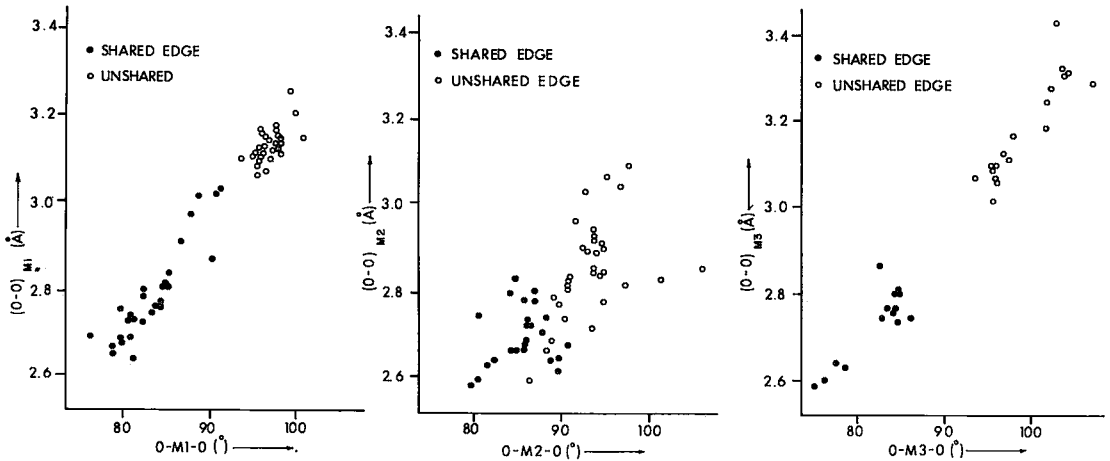


FIG. 51. Variation in length of the octahedral edges with the corresponding angles subtended at the central cation for the M1, M2 and M3 sites in the *Pnma* amphiboles.

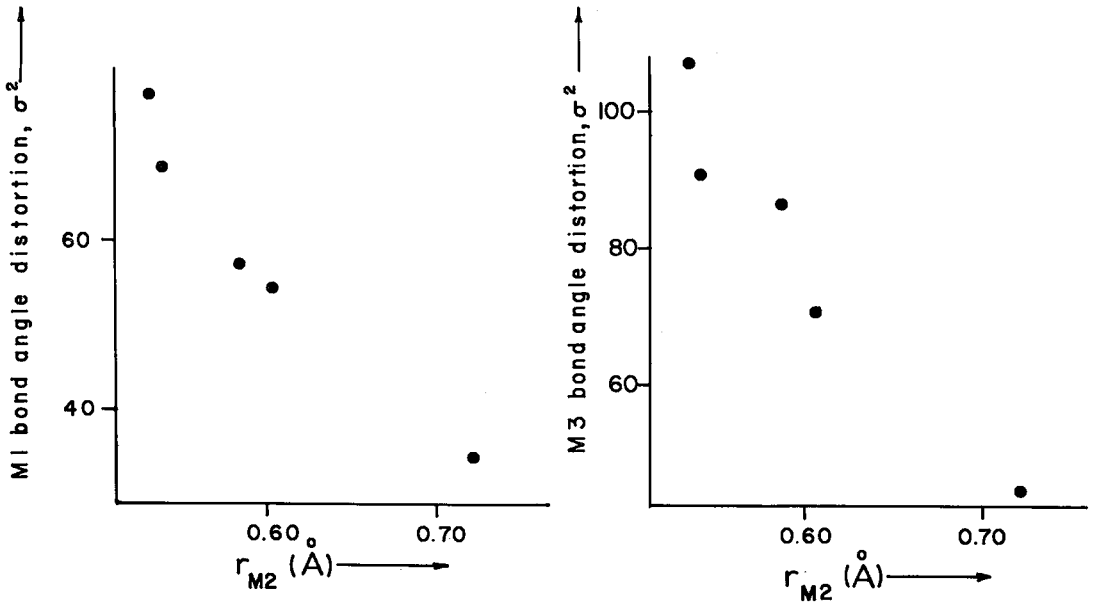


FIG. 52. Variation of the variance σ^2 in the octahedral angle for M1 and M3 with the mean ionic radius of the constituent M2 cations in the *Pnma* amphiboles.

the bond-length variations tend to minimize the deviations of the bond-valence sums from their ideal values. As is evident from Table 31, the M2 octahedron is far more distorted than the corresponding octahedra in tremolite(30) and fluor-tremolite(36), as expected for an amphibole with a high M4 occupancy of monovalent cations. Polyhedral elements shared between adjacent polyhedra are generally shorter

than the unshared elements, presumably as a result of cation-cation repulsion (Gibbs 1969), and the steric effects of the O4 bond-valence requirements significantly affect the interbond angles of the M2 octahedron, as shown in Table 31.

THE M(4) SITE

The M(4) site is situated at the junction of